Analysis of Viscoelastic Flow by a Radial Basis Function Networks Method

D. Ho-Minh, N. Mai-Duy and T. Tran-Cong

Faculty of Engineering and Surveying
University of Southern Queensland, Toowoomba, QLD 4350, AUSTRALIA

Abstract

This paper presents a new mesh-free numerical method based on MultiQuadric (MQ) Radial Basis Function Networks (RBFNs) for the analysis of viscoelastic flows. The method uses universal approximation RBFNs to represent the numerical solution of Partial Differential Equations (PDEs) governing viscoelastic flows. The main advantages of the method are its mesh-free nature and ease of implementation. The working of the method is demonstrated in detail with the simulation of the viscoelastic flow through straight (Poiseuille flow) and corrugated tubes. In the case of corrugated tube flow, the irregularly shaped domain is extended to a regularly shaped one in order to simplify the pre-processing. The method achieves the Weissenberg number of at least up to 100 for the Poiseuille flow of UCM and Oldroyd-B fluids using a collocation density of 6×6 and about 4 for the corrugated tube flow of Oldroyd-B fluid using a collocation density of 13×25.

Introduction

The Finite Difference Method (FDM) [24, 26], the Finite Element Method (FEM) [7, 12, 30], the Boundary Element Method (BEM) [2, 21] and the Finite Volume Method (FVM) [13, 20] are among the principal methods for numerical solution of problems in continuum mechanics. These methods are based on some discretisation of the domain of analysis into a number of elements and have underpinned enormous progress. However, mesh generation especially for 3D problems presents significant difficulties in the analysis of engineering problems. Considerable effort has been devoted in recent years to the development of the so-called meshless methods. A number of meshless methods have been developed such as Element Free Galerkin method (EFG) [3], Reproducing Kernel Particle Method (RKPM) [15], Finite Point Method (FPM) [19], Meshless Local Petrov-Galerkin method (MLPG) [1], neural network based method and several others. Neural Networks (NNs), which are capable of univesal approximation, have found applications in many disciplines [11]. Particularly, the concept of solving PDEs using NNs was first introduced by Kansa [14] in the case of Radial Basis Function Networks (RBFNs) and by Dissanayake and Phan-Thien [8] in the case of Multilayer Perceptrons (MPs). Typically for a NN-based method, each variable in the governing equations is represented by a NN and then the training process is employed to make the networks satisfy the PDEs and also boundary conditions. It should be emphasized that this procedure requires only a set of unstructured discrete collocation points and in that sense the NN-based method can be regarded as a mesh-less numerical method. Since these original works, further interesting developments were reported, including Takeuchi and Kosugi [27] in the MPs case and Kansa [14]; Dubal [9]; Sharan et al [25]; Zerroukat et al [28] and Mai-Duy and Tran-Cong [16, 18] in the RBFNs case. For example, the RBF approximation schemes using MultiQuadric basis function (MQ) were verified successfully for numerical solution of elliptic PDEs (Laplace, Poisson and biharmonic equations) by Sharan et al [25] and heat tranfer problems by Zerroukat et al [28]. Recently, Mai-Duy and Tran-Cong [16, 18] proposed new methods based on MQ-RBFNs for approximation of functions and numerical solution of ODEs and elliptic PDEs. The so-called Direct RBFN (DRBFN) and Indirect RBFN (IRBFN) methods were studied and it was found that the IRBFN method yields a superior accuracy in comparison with the DRBFN and also with other NN-based methods [16]. Furthermore, the IRBFN method has also been developed successfully for the analysis of viscous flows [17]. In this paper, the IRBFN method is further developed for numerical solution of the PDEs governing viscoelastic flow problems which are challenging due to a combination of ellipticity and hyperbolicity in the governing equations. The paper is organised as follows. In the second section, the governing equations for the flow of UCM and Oldroyd-B fluids are reviewed. In the third section, numerical formulation of viscoelastic flow problems using IRBFNs is presented in which the IRBFN formulation for axisymmetric flow problems is given in detail. The fourth section describes numerical results obtained by the IRBFN method for the simulation of the flow through a straight tube (test problem) and a corrugated tube (benchmark problem). Finally, the last section gives some concluding remarks.

Governing equations

The flow is assumed to be isothermal, creeping, and incompressible for which the equations of motion are

$$\nabla \cdot \boldsymbol{\sigma} = \mathbf{0}, \quad \mathbf{x} \in V, \tag{1}$$

$$\nabla \cdot \mathbf{u} = \mathbf{0}, \quad \mathbf{x} \in V, \tag{2}$$

where $(\boldsymbol{\sigma})$ is the total stress tensor and $\mathbf{u}$ is the velocity vector. For the Oldroyd-B model, the total stress tensor $(\boldsymbol{\sigma})$ can be written as

$$\boldsymbol{\sigma} = -P\mathbf{1} + 2\eta_n \mathbf{D} + \boldsymbol{\tau}, \tag{3}$$

where P is the pressure, $\mathbf{1}$ is the unit tensor, η_n is the "Newtonian contribution" viscosity, $\mathbf{D}$ is the rate of strain tensor and $(\boldsymbol{\tau})$ is the extra stress tensor obeying

$$\lambda \frac{\triangle \boldsymbol{\tau}}{\triangle t} + \boldsymbol{\tau} = 2\eta_p \mathbf{D}, \tag{4}$$

in which λ is the relaxation time, η_p is the "polymer contribution" viscosity and $\frac{\triangle \boldsymbol{\tau}}{\triangle t}$ is the upper convected derivative of $\boldsymbol{\tau}$ defined by

$$\frac{\triangle \boldsymbol{\tau}}{\triangle t} = \frac{\partial \boldsymbol{\tau}}{\partial t} + \mathbf{u} \cdot \nabla \boldsymbol{\tau} - \nabla \boldsymbol{\tau} \cdot \mathbf{u} - \boldsymbol{\tau} \cdot \nabla \mathbf{u}^T. \tag{5}$$

The constants η_n and η_p are defined by the relationships

$$\eta = \eta_n + \eta_p, \quad \alpha = \frac{\eta_n}{\eta_n + \eta_p}.$$

If $\eta_n = 0$, the Oldroyd-B model reduces to the UCM model. To get the Newtonian model we simply set $\lambda = 0$.

Numerical formulation based on radial basis function networks

The basic derivation of the present IRBFN method is given elsewhere [16, 18]. In this section, the method is briefly summarized for convenience and then developed further for the numerical solution of the PDEs governing viscoelastic flows. Each variable in the governing equations is represented by a RBFN based on the indirect approach [16]. For example, considering a variable ψ in the governing equations, the second order derivatives of ψ with respect to x_j are decomposed into radial basis functions, followed by successive symbolic integrations to obtain a closed form expression for lower order derivatives and finally the function(s) itself as follows

$$\psi_{,jj}(x) = \sum_{i=1}^{m} w^{(i)} g^{(i)}(x), \tag{6}$$

$$\psi_{,j}(x) = \int \psi_{,jj}(x)dx_j = \sum_{i=1}^{m} w^{(i)} \int g^{(i)}(x)dx_j, \tag{7}$$

$$\psi^{j}(x) = \int \psi_{,j}(x)dx_j$$
$$= \sum_{i=1}^{m} w^{(i)} \int \left(\int g^{(i)}(x)dx_j \right) dx_j. \tag{8}$$

where a superscript within parentheses, e.g. (i), is used to denote elements of a set under consideration, e.g. a set of RBFs; m is the number of RBFs; $\{w^{(i)}\}_{i=1}^{m}$ is the set of weights and $\{g^{(i)}\}_{i=1}^{m}$ is the set of radial basis functions. In this work the chosen RBF is the Multiquadric (MQ) given by

$$g^{(i)}(x) = g^{(i)}(\|x - c^{(i)}\|) = g^{(i)}(r) = \sqrt{r^2 + a^{(i)2}} \tag{9}$$

where x is the collocation point, $c^{(i)}$ is the ith centre, r is the distance between the collocation point and the ith centre and $a^{(i)}$ is the ith RBF width. It should be noted that the RBF width affects the performance of RBFNs, however no general mathematical theory has been developed for determining its optimal value [24]. In the present work the RBF width is determined based on the following relation

$$a^{(i)} = \beta d^{(i)}, \tag{10}$$

where β is a factor, $\beta > 0$, and $d^{(i)}$ is the distance from the ith centre to the nearest centre. The closed form variable representations thus obtained are then substituted into the governing equations and boundary conditions to discretise the system via the mechanism of point collocation at $\{x^{(i)}\}_{i=1}^{n}$ where n is the number of collocation points. Once the centres and widths are chosen in advance, the unknowns of the system of algebraic equations obtained contain only RBF weights. The method does not require any kind of "finite element-type" discretisation of the domain and its boundary. Instead, two sets of random points distributed throughout the domain and on the boundary are required (Figure 1). The first set defines the centres of the RBFs and the second defines the collocation points. The two sets of points can be different, however experience shows that if the two sets are the same better results are obtained. The application of the method to the present problem, i.e. (1)-(5) together with boundary conditions, results in the following sum squared error (SSE), which is to be minimised in the sense of the general least squares principle,

$$SSE = SSE_1 + SSE_2 + SSE_3, \tag{11}$$

where SSE_1, SSE_2 and SSE_3 are the sums of squared errors which are employed to ensure that the neural networks satisfy the governing equations, the identity of networks associated with each variable in governing equations (e.g. the various networks representing the same variable ψ are forced to be equal resulting in a constraint equation) and the boundary conditions respectively. The form of SSE_3 depends on the problem to be solved while SSE_1 and SSE_2 can be written in the general form provided that the governing equations are given. A nonlinear system of algebraic equations with unknowns RBF weights is thus obtained and can be solved by using a Picard-type scheme that consists of the following steps

- Guess the initial velocity for the first iteration (usually zero in the present work);

- Render the non-linear terms (namely $\mathbf{u} \cdot \nabla \tau, \nabla \tau \cdot \mathbf{u}, \tau \cdot \nabla \mathbf{u}^T$ in the upper convected derivatives) linear by using the current estimate of the velocity field;

- Solve the linear system obtained in the sense of the general linear least squares principle for the new estimate of the velocity field;

- Check for convergence. The convergence measure (CM) at the kth iteration is defined as follows

$$CM = \sqrt{\frac{\sum_{j=1}^{3} \sum_{i=1}^{n} (u_j^k(x^{(i)}) - u_j^{k-1}(x^{(i)}))^2}{\sum_{j=1}^{3} \sum_{i=1}^{n} (u_j^k(x^{(i)}))^2}}. \tag{12}$$

The solution procedure is terminated when $CM < tol$, where tol is a set tolerance;

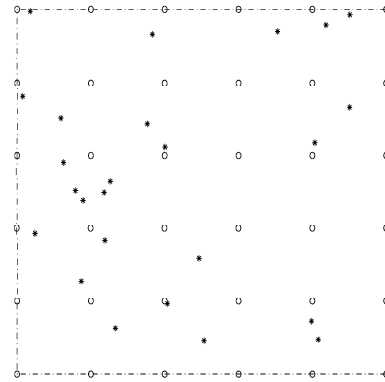- If not yet converged, repeat from step 2;

- If converged, stop.

Figure 1: RBF centres and discretisation with collocation points. Legends ∘: RBF centre and ∗: collocation point. RBF centres are regularly distributed for best results while collocation points can be random.

In the following, the working of the present IRBFN method is demonstrated in detail with the simulation of viscoelastic flows through straight and corrugated tubes. In the case of axisymmetric flow problems, the SSE_1 and SSE_2 take the following forms

$$\begin{aligned}
SSE_1 = & \sum_{(i) \in \Omega} \left[E_{11}^{(i)} \right]^2 + \sum_{(i) \in \Omega} \left[E_{12}^{(i)} \right]^2 + \sum_{(i) \in \Omega} \left[E_{13}^{(i)} \right]^2 \\
& + \sum_{(i) \in \Omega} \left[E_{14}^{(i)} \right]^2 + \sum_{(i) \in \Omega} \left[E_{15}^{(i)} \right]^2 + \sum_{(i) \in \Omega} \left[E_{16}^{(i)} \right]^2 \\
& + \sum_{(i) \in \Omega} \left[E_{17}^{(i)} \right]^2.
\end{aligned} \tag{13}$$

where:

$$E_{11}^{(i)} = \eta_n \left[u_{r,rr}^{(i)} + \frac{u_{r,r}^{(i)}}{r^{(i)}} + u_{r,zz}^{(i)} - \frac{u_r^{r(i)}}{r^{(i)2}} \right] - P_{,r}^{(i)} + \tau_{rr,r}^{(i)}$$

$$+ \quad \tau_{rz,z}^{(i)} + \frac{\tau_{rr}^{r(i)} - \tau_{\theta\theta}^{r(i)}}{r^{(i)}}. \tag{14}$$

$$E_{12}^{(i)} = \eta_n \left[u_{z,rr}^{(i)} + \frac{u_{z,r}^{(i)}}{r^{(i)}} + u_{z,zz}^{(i)} \right] - P_{,z}^{(i)} + \tau_{rz,r}^{(i)}$$

$$+ \quad \frac{\tau_{rz}^{r(i)}}{r^{(i)}} + \tau_{zz,z}^{(i)}. \tag{15}$$

$$E_{13}^{(i)} = u_{r,r}^{(i)} + \frac{u_r^{r(i)}}{r^{(i)}} + u_{z,z}^{(i)}. \tag{16}$$

$$E_{14}^{(i)} = \tau_{rr}^{r(i)} + \lambda \left[u_r^{r(i)} \tau_{rr,r}^{(i)} + u_z^{r(i)} \tau_{rr,z}^{(i)} - 2u_{r,r}^{(i)} \tau_{rr}^{r(i)} \right.$$

$$- \quad 2u_{r,z}^{(i)} \tau_{rz}^{r(i)} \right] - 2\eta_p u_{r,r}^{(i)}. \tag{17}$$

$$E_{15}^{(i)} = \tau_{rz}^{r(i)} + \lambda \left[u_r^{r(i)} \tau_{rz,r}^{(i)} + u_z^{r(i)} \tau_{rz,z}^{(i)} - u_{r,r}^{(i)} \tau_{rz}^{r(i)} - u_{r,z}^{(i)} \tau_{zz}^{r(i)} \right.$$

$$- \quad u_{z,r}^{(i)} \tau_{rr}^{r(i)} - u_{z,z}^{(i)} \tau_{rz}^{r(i)} \right] - \eta_p \left[u_{r,z}^{(i)} + u_{z,r}^{(i)} \right]. \tag{18}$$

$$E_{16}^{(i)} = \tau_{zz}^{r(i)} + \lambda \left[u_r^{r(i)} \tau_{zz,r}^{(i)} + u_z^{r(i)} \tau_{zz,z}^{(i)} - 2u_{z,r}^{(i)} \tau_{rz}^{r(i)} \right.$$

$$- \quad 2u_{z,z}^{(i)} \tau_{zz}^{r(i)} \right] - 2\eta_p u_{z,z}^{(i)}. \tag{19}$$

$$E_{17}^{(i)} = \tau_{\theta\theta}^{r(i)} + \lambda \left[u_r^{r(i)} \tau_{\theta\theta,r}^{(i)} + u_z^{r(i)} \tau_{\theta\theta,z}^{(i)} - 2\frac{u_r^{r(i)}}{r^{(i)}} \tau_{\theta\theta}^{r(i)} \right]$$

$$- \quad 2\eta_p \frac{u_r^{r(i)}}{r^{(i)}}. \tag{20}$$

$$SSE_2 = \sum_{(i)\in\Omega} \left\{ u_r^{r(i)} - u_r^{z(i)} \right\}^2 + \sum_{(i)\in\Omega} \left\{ u_z^{r(i)} - u_z^{z(i)} \right\}^2$$

$$+ \quad \sum_{(i)\in\Omega} \left\{ P^{r(i)} - P^{z(i)} \right\}^2 + \sum_{(i)\in\Omega} \left\{ \tau_{rr}^{r(i)} - \tau_{rr}^{z(i)} \right\}^2$$

$$+ \quad \sum_{(i)\in\Omega} \left\{ \tau_{rz}^{r(i)} - \tau_{rz}^{z(i)} \right\}^2 + \sum_{(i)\in\Omega} \left\{ \tau_{zz}^{r(i)} - \tau_{zz}^{z(i)} \right\}^2$$

$$+ \quad \sum_{(i)\in\Omega} \left\{ \tau_{\theta\theta}^{r(i)} - \tau_{\theta\theta}^{z(i)} \right\}^2. \tag{21}$$

The SSE_3 will be given later as it depends on the problem to be solved.

Numerical examples

The flow through straight and corrugated tubes is chosen and simulated here to verify the IRBFN method. In the following numerical examples, the tolerance for the convergence test is set to $5e - 3$.

A simple test problem - Axisymmetric Poiseuille flow

The problem of axisymmetric Poiseuille flow of UCM and Oldroyd-B ($\alpha = 1/9$) fluids is considered here. Dimensionless variables are introduced by scaling lengths with the radius of the tube R, velocity components with the maximum speed U (on the centreline) and stress components and pressure with $\eta U/R$. The closed form solution is given by

$$u_{ze} = 1 - r^2, \quad u_{re} = 0, \tag{22}$$

$$\tau_{zze} = W_e(1-\alpha)\left(\frac{\partial u_{ze}}{\partial r}\right)^2, \quad \tau_{rze} = (1-\alpha)\frac{\partial u_{ze}}{\partial r}, \quad \tau_{rre} = 0, \tag{23}$$

where $W_e = 2\lambda U/R = \lambda\dot{\gamma}$ is the Weissenberg number in which $\dot{\gamma}$ is the shear rate at the wall. Owing to axisymmetry, only one

half of the fluid domain with the dimension 1×1 is considered. At the inlet and the outlet, Dirichlet boundary conditions for the velocity and Neumann boundary conditions for the extra stress are imposed. No-slip conditions are enforced on the solid boundary and symmetry conditions are specified on the centre line. Hence, for this problem, the SSE_3 takes the form

$$SSE_3 = \sum_{(i)\in I} \left\{ u_r^{r(i)} \right\}^2 + \sum_{(i)\in I} \left[u_z^{r(i)} - \left(1 - r^{(i)2}\right) \right]^2$$

$$+ \quad \sum_{(i)\in I} \left\{ \tau_{rr,z}^{(i)} \right\}^2 + \sum_{(i)\in I} \left\{ \tau_{rz,z}^{(i)} \right\}^2 + \sum_{(i)\in I} \left\{ \tau_{zz,z}^{(i)} \right\}^2$$

$$+ \quad \sum_{(i)\in O} \left\{ u_r^{r(i)} \right\}^2 + \sum_{(i)\in O} \left[u_z^{r(i)} - \left(1 - r^{(i)2}\right) \right]^2$$

$$+ \quad \sum_{(i)\in O} \left\{ \tau_{rr,z}^{(i)} \right\}^2 + \sum_{(i)\in O} \left\{ \tau_{rz,z}^{(i)} \right\}^2 + \sum_{(i)\in O} \left\{ \tau_{zz,z}^{(i)} \right\}^2$$

$$+ \quad \sum_{(i)\in W} \left\{ u_r^{r(i)} \right\}^2 + \sum_{(i)\in W} \left\{ u_z^{r(i)} \right\}^2 + \sum_{(i)\in C} \left\{ u_r^{r(i)} \right\}^2$$

$$+ \quad \sum_{(i)\in C} \left\{ \tau_{rz}^{r(i)} \right\}^2. \tag{24}$$

where I, O, W, C stand for Inlet, Outlet, Wall, Centreline, respectively.

The fluid flow is simulated numerically by the present IRBFN method. The quality of the solution is measured with the norm of the error of the velocity field denoted by $N_e u$ and of the stress field denoted by $N_e \tau$. The norm of the error of the velocity field for instance is defined as

$$N_e u = \sqrt{\frac{\sum_{i=1}^n [(u_r(x^{(i)}) - u_{re}(x^{(i)}))^2 + (u_z(x^{(i)}) - u_{ze}(x^{(i)}))^2]}{\sum_{i=1}^n [(u_{re}(x^{(i)}))^2 + (u_{ze}(x^{(i)}))^2]}}. \tag{25}$$

As mentioned above, the RBFN solution depends on the value of the RBF width β. Two studies of the parameter β are carried out using a uniform centre density of 6×6. The first is to investigate the effect of β on the quality of the solution at $W_e = 10$. The value of β is varied from 1 to 10 with an increment of 1. The method is convergent for all values of β with a high accuracy as shown in Table 1. The second study is to investigate the convergence behaviour with respect to the Weissenberg number. Table 2 presents the error norms $N_e u$ and $N_e \tau$ of the solution of Poiseuille flow at $\beta = 9$ for some Weissenberg numbers. The present method achieves up to at least $W_e = 100$ for both UCM and Oldroyd-B models using very low centre density of 6×6. The stress obtained at $W_e = 100$ on the middle plane is displayed in Figure 2 showing good agreement with the exact solution.

A benchmark problem - Corrugated tube flow

Due to the fact that the corrugated tube has converging-diverging sections, smooth boundaries and also no inflow or outflow boundaries, the flow in corrugated tube was suggested as a standard test problem at the $4th$ Workshop on Numerical Methods in Non-Newtonian Fluid Mechanics, held at Spa, Belgium in 1985 [5]. The problem has been studied by several different numerical methods, e.g. pseudospectral finite difference method (PSFD) and pseudospectral cylindrical finite difference method (PCFD) by Pilitsis and Beris [22], EEME by Burdette et al [5] and BEM by Zheng et al [29]. The radius of the undulating tube along the z-axis (Figure 3a) is given by

$$R = \bar{R}\left[1 - a\cos\left(\frac{2\pi z}{L}\right)\right], \tag{26}$$

where $\bar{R}$ is the mean radius of the tube, a is the amplitude of the undulation and L is the corrugation wavelength. The flow is

β	1	2	3	4	5
$N_e u$	$8.63e-4$	$5.61e-4$	$2.33e-4$	$6.42e-5$	$1.94e-5$
β	6	7	8	9	10
$N_e u$	$1.18e-5$	$3.54e-6$	$6.97e-6$	$8.84e-6$	$1.13e-5$

Table 1: Poiseuille flow, UCM model, centre density of 6×6, $W_e = 10$: Effect of β on the quality of the solution (error norm $N_e u$).

W_e	1	20	40	60	80	100
$N_e u$	$2.05e-5$	$2.66e-5$	$1.85e-4$	$4.22e-4$	$1.43e-3$	$1.90e-3$
$N_e \tau$	$6.08e-6$	$1.73e-4$	$3.13e-4$	$6.52e-4$	$2.56e-3$	$3.38e-3$

Table 2: Poiseuille flow, UCM model, centre density of 6×6: Error norms of the solution of Poiseuille flow at $\beta = 9.0$ for some Weissenberg numbers.
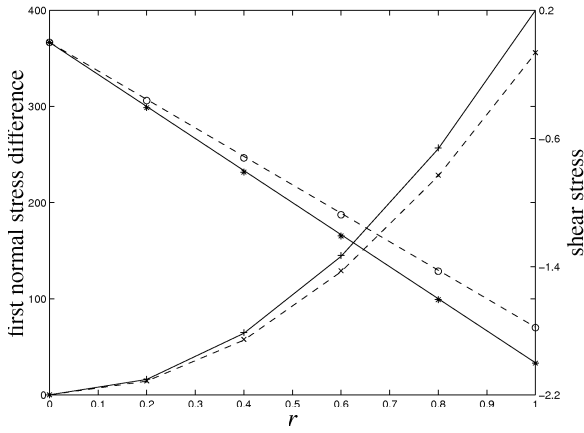

Figure 2: Axisymmetric Poiseuille flow of UCM and Oldroyd-B fluids at $W_e = 100$ using centre density of 6×6: The exact solution, computed first normal stress difference and computed shear stress on a middle plane are denoted by {solid line, +, *} and {dashed line, ×, o} for UCM and Oldroyd-B fluids, respectively.

Figure 3: Corrugated tube problem.

assumed to be axisymmetric and periodic with wavelength L, so that only the reduced domain shown in Figure 3b is considered. At the inlet and the outlet, the periodicity conditions for the velocity, velocity gradient and extra stress are employed. No-slip conditions and the symmetric conditions are imposed on the solid boundary and the centreline respectively. The pressure difference between the inlet and the outlet ΔP together with a reference value of the pressure are also enforced. The SSE_3 now becomes

$$
\begin{aligned}
SSE_3 &= \sum_{(i) \in I, (j) \in O} \left\{ u_r^{r(i)} - u_r^{r(j)} \right\}^2 + \sum_{(i) \in I, (j) \in O} \left\{ u_z^{r(i)} - u_z^{r(j)} \right\}^2 \\
&+ \sum_{(i) \in I, (j) \in O} \left\{ u_{r,r}^{r(i)} - u_{r,r}^{r(j)} \right\}^2 + \sum_{(i) \in I, (j) \in O} \left\{ u_{r,z}^{r(i)} - u_{r,z}^{r(j)} \right\}^2 \\
&+ \sum_{(i) \in I, (j) \in O} \left\{ u_{z,r}^{r(i)} - u_{z,r}^{r(j)} \right\}^2 + \sum_{(i) \in I, (j) \in O} \left\{ u_{z,z}^{r(i)} - u_{z,z}^{r(j)} \right\}^2 \\
&+ \sum_{(i) \in I, (j) \in O} \left\{ \tau_{rr}^{r(i)} - \tau_{rr}^{r(j)} \right\}^2 + \sum_{(i) \in I, (j) \in O} \left\{ \tau_{rz}^{r(i)} - \tau_{rz}^{r(j)} \right\}^2 \\
&+ \sum_{(i) \in I, (j) \in O} \left\{ \tau_{zz}^{r(i)} - \tau_{zz}^{r(j)} \right\}^2 + \sum_{(i) \in I, (j) \in O} \left\{ \tau_{\theta\theta}^{r(i)} - \tau_{\theta\theta}^{r(j)} \right\}^2 \\
&+ \sum_{(i) \in W} \left\{ u_r^{r(i)} \right\}^2 + \sum_{(i) \in W} \left\{ u_z^{r(i)} \right\}^2 + \sum_{(i) \in C} \left\{ u_r^{r(i)} \right\}^2
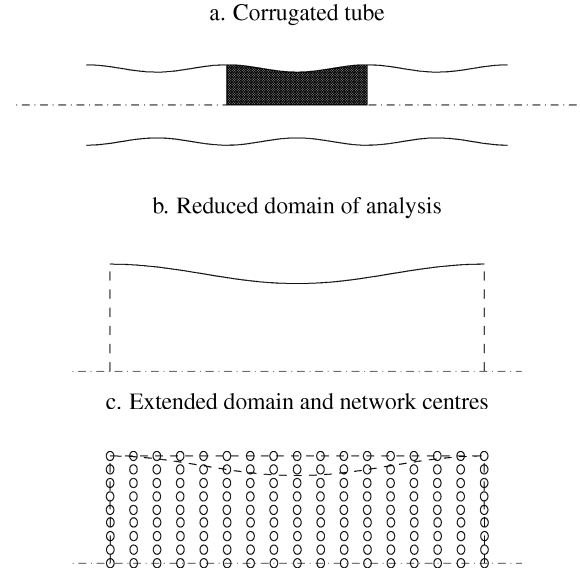\end{aligned}
$$

$$
+ \sum_{(i) \in C} \left\{ \tau_{rz}^{r(i)} \right\}^2 + \sum_{(i) \in I, (j) \in O} \left\{ P^{r(i)} - P^{r(j)} - \Delta P \right\}^2
$$

$$
+ \left\{ P^{r(i)} \right\}^2_{r^{(i)}=0, z^{(i)}=0}. \tag{27}
$$

where I, O, W, C stand for Inlet, Outlet, Wall, Centreline, respectively.

The governing equations here are made dimensionless by scaling lengths by $\bar{R}$, velocity components by $Q/\bar{R}^2$ and stress components and pressure by $\eta Q/\bar{R}^3$ where Q is the flow rate through the tube. Following Pilitsis and Beris [29], the importance of elastic effects is measured by the Weissenberg number defined as

$$
W_e = \frac{\lambda Q}{\bar{R}^3}, \tag{28}
$$

where Q is the flow rate. The quantity of interest is the flow resistance, fRe, defined by

$$
fRe = \frac{2\pi \Delta P \bar{R}^4}{L \eta Q}. \tag{29}
$$

It can be seen that if the networks are trained to satisfy the governing equations on the extended domain Ω^* which contains the original domain Ω and also the given boundary conditions, the solution obtained is also the solution to the problem on the original domain Ω. Hence, in order to make the pre-processing

more convenient, the non-rectangular original domain can be extended into a number of rectangular subdomains provided that these subdomains together can cover entirely the original domain Ω. For the present problem, the undulated domain is extended into a rectangular one as shown in Figure 3c. Then, a set of centres can be easily generated using the intersection points of the rectangular gridlines (Figure 3c) while a set of collocation points consists of two parts. The first part is the same as the set of centres where the governing equations are enforced and the second part where the boundary conditions are enforced can be simply chosen as the intersection points between the curved boundary and the rectangular gridlines through the centres.
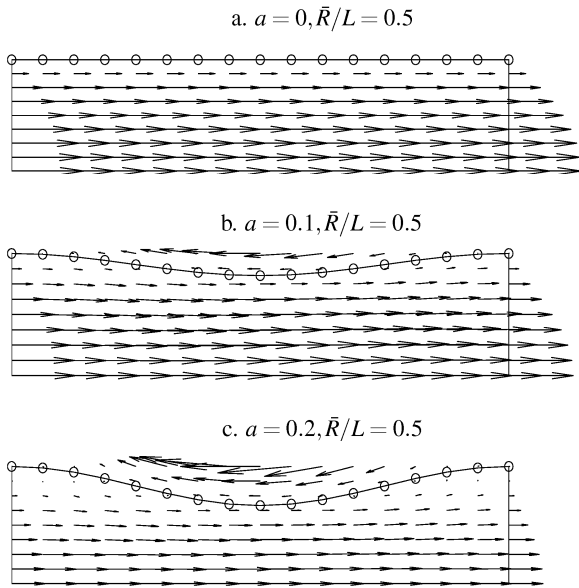
a. $a = 0, \bar{R}/L = 0.5$

b. $a = 0.1, \bar{R}/L = 0.5$

c. $a = 0.2, \bar{R}/L = 0.5$

Figure 4: Corrugated tube problem, Newtonian fluid, $\beta = 10$, centre density of 9×17: Velocity vector fields corresponding to different undulation amplitudes.
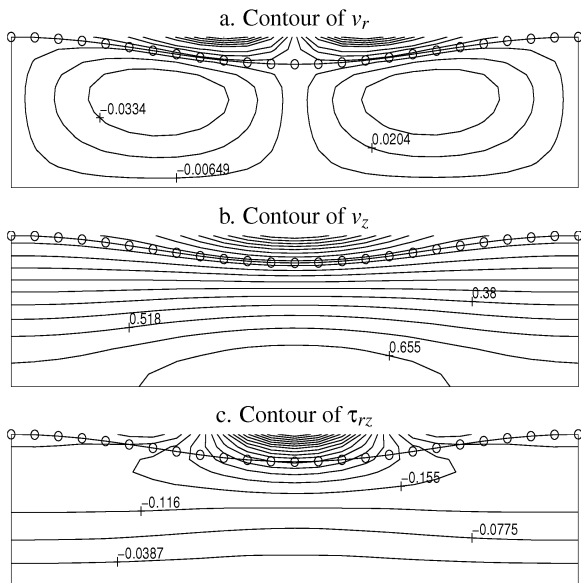
a. Contour of v_r

b. Contour of v_z

c. Contour of τ_{rz}

Figure 5: Corrugated tube problem, Newtonian fluid, $\beta = 8$, centre density of 13×25: Contours of v_r, v_z and τ_{rz}.

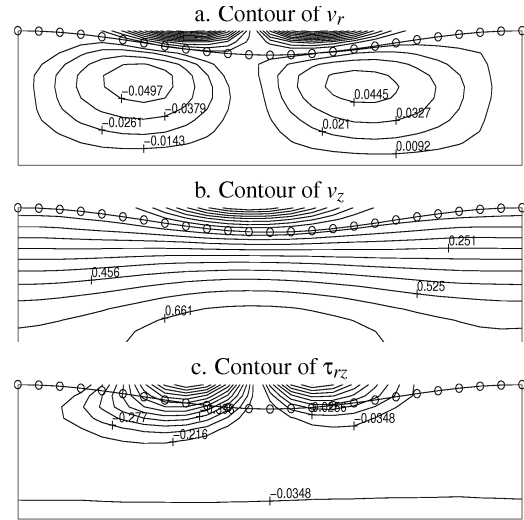a. Contour of v_r

b. Contour of v_z

c. Contour of τ_{rz}

Figure 6: Corrugated tube problem, Oldroyd-B fluid, $W_e = 2.0$, $\beta = 8$, centre density of 13×25: Contours of v_r, v_z and τ_{rz}.

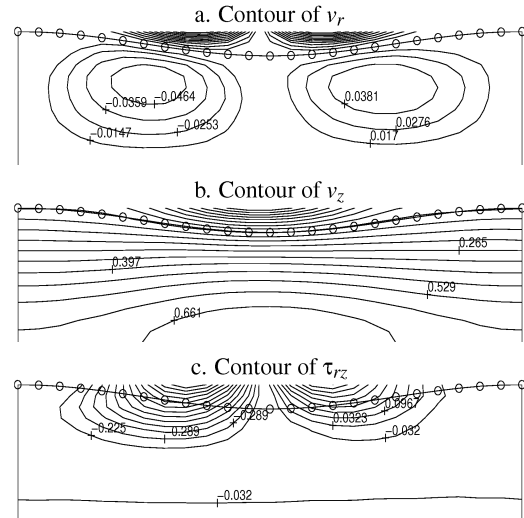a. Contour of v_r

b. Contour of v_z

c. Contour of τ_{rz}

Figure 7: Corrugated tube problem, Oldroyd-B fluid, $W_e = 3.0$, $\beta = 8$, centre density of 13×25: Contours of v_r, v_z and τ_{rz}.

The present IRBFN method for numerical solution of the corrugated tube flow is first verified with the Newtonian fluid. A number of undulation amplitudes, including the special case of straight tube, are studied. The flow resistances fRe obtained by the present method using the centre density of 9×17 are compared with those from other methods, which shows a good agreement. In the case of the straight tube ($a = 0$ and $\bar{R}/L = 0.5$), the error between the present IRBFN and the exact solution is $2.41e - 4\%$. For the corrugated tube ($a = [0.1, 0.2]$ and $\bar{R}/L = 0.5$) the difference between the present IRBFN results and the results of PCFD [22] is within about 3% (Table 3). The corresponding velocity vector fields are displayed in Figure 4. Attention is now focused on the flow of an Oldroyd-B fluid ($\alpha = 0.85$) through the corrugated tube ($a = 0.1$ and $\bar{R}/L = 0.5$). Three centre densities of 9×17, 11×21 and 13×25 are employed to simulate the corrugated tube flow. In the case of Newtonian fluid, the contours of u_r, u_z and τ_{rz} are symmetric about the narrowest section (Figure 5). Symmetric behaviour also applies to other variables except pressure, however for brevity they

Geometries	IRBFN	Analytical	BEM	PCFD	EEMM	Pertb
$a = 0.0, \bar{R}/L = 0.5$	16.0000	16	15.9999	-	-	-
$a = 0.1, \bar{R}/L = 0.5$	17.7757	-	17.73	17.75	17.71	17.85
$a = 0.2, \bar{R}/L = 0.5$	23.4234	-	23.22	23.28	-	24.16

Table 3: Corrugated tube problem, Newtonian fluid, centre density of 9×17, $\beta = 10$: Comparison of the flow resistance fRe between methods. Note that the results from other methods such as the Perturbation (Pertb) are extracted from the paper by Zheng et al [30].

	$9 \times 17, \beta = 10$	$11 \times 21, \beta = 9$	$13 \times 25, \beta = 8$
$W_e = 0$	17.7757	17.7318	17.7354
$W_e = 1$	17.6004	17.6969	17.7075
$W_e = 2$	17.6886	17.8184	17.7409
$W_e = 3.01$	17.6366	17.4296	17.7580
$W_e = 4.15$	17.0392	16.9804	17.1408

Table 4: Corrugated tube problem, Oldroyd-B fluid ($\alpha = 0.85$), the flow resistance fRe obtained with three centre densities of 9×17, 11×21 and 13×25.
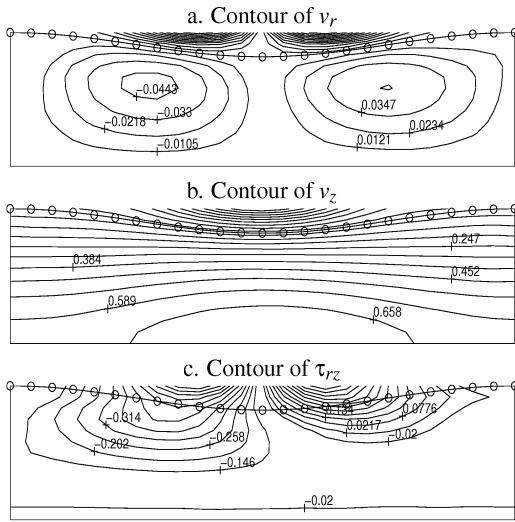

Figure 8: Corrugated tube problem, Oldroyd-B fluid, $W_e = 4.14$, $\beta = 8$, centre density of 13×25: Contours of v_r, v_z and τ_{rz}.

are not displayed. When the elasticity component is introduced (i.e. $\lambda > 0$), the symmetry about the narrowest section is destroyed. For example, the contours of τ_{rz} are clearly unsymmetric as shown in Figures 6 - 8, where it can be seen that the stress level increases with increasing W_e number. It is observed that the velocity vector field does not change by much in comparison with that of Newtonian fluid. Table 4 displays the flow resistances fRe obtained with three centre densities, which are a bit lower than the results of about 17.7 obtained by the PCFD method, however the difference is still within about 3%. The IRBFN result corresponding to the highest density (13×25) is closer to the PCFD result than that of the lowest density (9×17) as expected.

Conclusions remarks

This paper presents the successful development and implementation of the indirect multiquadric radial basis function networks method for numerical solution of viscoelastic flows. The method requires only two sets of discrete data points (i.e. the set of centres and the set of collocation points) to discretise the governing equations and the boundary conditions and of-

fers the advantage of being mesh-free. Although the choice of RBF width is still simple in the present work, numerical examples studied showed that the results obtained are close to the exact and benchmark solutions. Since the RBF widths are non-optimal and due to an evolution of the solution during the iterative process, the RBF widths should be adaptive. A method for determining the optimal value of RBF width in order to exploit the capability of the universal RBF approximation could be investigated in future work.

References

[1] Atluri, S.N. and Zhu, T., A new meshless local petrov-galerkin (mlpg) approach in computational mechanics, *Computational Mechanics*, **22**, 1998 , 117–127.

[2] Banerjee, P.K. and Butterfield, R., *Boundary Element Methods in Engineering Science*, McGraw-Hill, London, 1981.

[3] Belytschko, T., Lu, Y. and Gu, L., Element free Galerkin method, *International Journal for Numerical Methods in Engineering*, **37**, 1994, 229–256.

[4] Brebbia, C.A., Telles, J.C.F. and Wrobel, L.C., *Boundary Elements: An Introductory Course*, Computational Mechanics Publications, Southampton, 1984.

[5] Burdette, S.R., Coates, P.J., Armstrong, R.C. and Brown, R.A., Calculations of viscoelastic flow through an axisymmetric corrugated tube using the explicitly elliptic momentum equation formulation (EEME), *Journal of Non-Newtonian Fluid Mechanics*, **33**, 1989 , 1-23.

[6] Cook, R.D., Malkus, D.S. and Plesha, M.E., *Concepts and Applications of Finite Element Analysis*, John Wiley and Sons, Toronto, 1989.

[7] Crochet, M.J., Davies, A.R. and Walters, K., *Numerical Simulation of Non-Newtonian Flow*, Elsevier, Amsterdam, 1984.

[8] Dissanayake, M.W.M.G. and Phan-Thien, N., Neural network based approximations for solving partial differential equations, *Communications in Numerical Methods in Engineering*, **10**, 1994, 195–201.

[9] Dubal, M.R., Domain decomposition and local refinement for multiquadric approximations. I: Second-order equations in one-dimension, *Journal of Applied Science and Computation*, **1(1)**, 1994, 146–171.

[10] Fletcher, C.A.J., *Computational Galerkin Methods*, Springer–Verlag, New York, 1984.

[11] Haykin, S., *Neural Networks: A Comprehensive Foundation*, Prentice-Hall, New Jersey, 1999.

[12] Hughes, T.J.R., *The Finite Element Method*, Prentice–Hall, New Jersey, 1987.

[13] Huilgol, R.R. and Phan-Thien, N., *Fluid Mechanics of Viscoelasticity*, Elsevier, Amsterdam, 1997.

[14] Kansa, E.J., Multiquadrics- A scattered data approximation scheme with applications to computational fluid-dynamics-I. Surface approximations and partial derivative estimates, *Computers and Mathematics with Applications*, **19(8/9)**, 1990, 127–145.

[15] Liu, W. K., Jun, S. and Zhang, Y., Reproducing kernel particle methods, *International Journal for numerical Methods in Fluids*, **20**, 1995 , 1081–1106.

[16] Mai-Duy, N. and Tran-Cong, T., Numerical solution of differential equations using multiquadric radial basis function networks, *Neural Networks*, **14(2)**, 2001, 185–199.

[17] Mai-Duy, N. and Tran-Cong, T., Numerical solution of Navier-Stokes equations using multiquadric radial basis function networks, *International Journal for Numerical Methods in Fluids*, **37**, 2001, 65–86.

[18] Mai-Duy, N. and Tran-Cong, T., Mesh-free radial basis function network methods with domain decomposition for approximation of functions and numerical solution of Poisson's equations, *Engineering Analysis with Boundary Element*, **26(2)**,2002 , 133–156.

[19] Onate, E., Idelsohn, S., Zienkiewicz, O.C. and Taylor, R.L., A finite point method in computational mechanics, applications to convective transport and fluid flow, *International Journal for Numerical Methods in Engineering*, **39(22)**, 1996, 3839–3866.

[20] Patankar, S.V., *Numerical Heat Transfer and Fluid Flow*, McGraw-Hill, New York, 1980.

[21] Phan-Thien, N. and Kim, S., *Microstructures in Elastic Media Principles and Computational Methods*, Oxford University Press, New York, 1994.

[22] Pilitsis, S. and Beris, A.N., Calculations of steady-state viscoelastic flow in an undulating tube, *Journal of Non-Newtonian Fluid Mechanics*, **31**, 1989, 231–287.

[23] Reddy, J.N. and Gartling, D.K., *The Finite Element Method in Heat Transfer and Fluid Dynamics*, CRC Press, Boca Raton, 1987.

[24] Roache, P.J., *Fundamentals of Computational Fluid Dynamics*, Hermosa Publishers, Albuquerque, 1998.

[25] Sharan, M., Kansa, E.J. and Gupta, S., Application of the multiquadric method for numerical solution of elliptic partial differential equations, *Journal of Applied Science and Computation*, **84**, 1997, 275–302.

[26] Smith, G.D., *Numerical Solution of Partial Differential Equations: Finite Difference Methods*, Claredon Press, Oxford, 1978.

[27] Takeuchi, J. and Kosugi, Y., Neural network representation of finite element method, *Neural Networks*, **7(2)**, 1994, 389–395.

[28] Zerroukat, M.,Power, H. and Chen, C.S., A numerical method for heat transfer problems using collocation and radial basis functions, *International Journal for Numerical Methods in Engineering*, **42**, 1998, 1263–1278.

[29] Zheng, R., Phan-Thien, N., Tanner, R.I. and Bush, M.B., Numerical analysis of viscoelastic flow through a sinusoidally corrugated tube using a boundary element method, *Journal of Rheology*, **34(1)**, 1989, 79–102.

[30] Zienkiewicz, O.C. and Taylor, R.L., *The Finite Element Method*, McGraw-Hill, London, 1991.